# Mechanochemical regulation of oscillatory follicle cell dynamics in the developing *Drosophila* egg chamber

Sarita Koride[a], Li He[b], Li-Ping Xiong[c], Ganhui Lan[c], Denise J. Montell[d], and Sean X. Sun[e,f]
[a]Department of Chemical and Biomolecular Engineering, [e]Johns Hopkins Physical Sciences-Oncology Center, and [f]Department of Mechanical Engineering, Biomedical Engineering, Johns Hopkins University, Baltimore, MD 21218; [b]Howard Hughes Medical Institute, Department of Genetics, Harvard Medical School, Boston, MA 02115; [c]Department of Physics, George Washington University, Washington, DC 20052; [d]Department of Molecular, Cellular and Developmental Biology, University of California, Santa Barbara, Santa Barbara, CA 93106

**ABSTRACT** **During tissue elongation from stage 9 to stage 10 in *Drosophila* oogenesis, the egg chamber increases in length by ~1.7-fold while increasing in volume by eightfold. During these stages, spontaneous oscillations in the contraction of cell basal surfaces develop in a subset of follicle cells. This patterned activity is required for elongation of the egg chamber; however, the mechanisms generating the spatiotemporal pattern have been unclear. Here we use a combination of quantitative modeling and experimental perturbation to show that mechanochemical interactions are sufficient to generate oscillations of myosin contractile activity in the observed spatiotemporal pattern. We propose that follicle cells in the epithelial layer contract against pressure in the expanding egg chamber. As tension in the epithelial layer increases, Rho kinase signaling activates myosin assembly and contraction. The activation process is cooperative, leading to a limit cycle in the myosin dynamics. Our model produces asynchronous oscillations in follicle cell area and myosin content, consistent with experimental observations. In addition, we test the prediction that removal of the basal lamina will increase the average oscillation period. The model demonstrates that in principle, mechanochemical interactions are sufficient to drive patterning and morphogenesis, independent of patterned gene expression.**

**Monitoring Editor**
Leah Edelstein-Keshet
University of British Columbia

Received: Apr 17, 2014
Revised: May 29, 2014
Accepted: Jun 10, 2014

## INTRODUCTION

The *Drosophila* ovary is composed of strings of developing egg chambers of increasing size and maturity (Figure 1, A–D). Each egg chamber contains 16 germ cells surrounded by a monolayer of epithelial follicle cells. Egg chambers increase in volume over time while also becoming elongated. Follicle cell shape oscillations begin during stage 9 of development in a subset of cells near the center and correlate with increasing basal myosin content due to activation of Rho GTPase and Rho-associated protein kinase, ROCK (He, Wang, *et al.*, 2010). The maximal level of myosin activity and the number of cells undergoing oscillations increases during stage 9 until most of the epithelium shows high myosin activity at stage 10 (Figure 1, B–D). These observed oscillations in the basal surface area of follicle cells restrict the egg chamber width and thus promote tissue elongation and morphogenesis. Autonomous periodic oscillations have been explored in other areas in biology (Winfree, 1980; Goldbeter, 1996; Ferrel *et al.*, 2011). Here we propose a mechanochemical model of cell contractility in the developing epithelium and investigate the spatial and temporal patterns in these oscillations using a combination of experiments and modeling. The model couples contractile forces generated by cells with mechanical tension from the external environment, including both the underlying germline cells and the overlying basal lamina. The model predicts that a cell can adjust its contractile force in response to external forces, and in some parameter regimes, the interplay of external

This article was published online ahead of print in MBoC in Press (http://www.molbiolcell.org/cgi/doi/10.1091/mbc.E14-04-0875) on June 18, 2014.

Address correspondence to: Sean X. Sun (ssun@jhu.edu).

Abbreviations used: A-P, anterior-posterior; D-V, dorsal-ventral.





Supplemental Material can be found at:
http://www.molbiolcell.org/content/suppl/2014/06/16/mbc.E14-04-0875v1.DC1

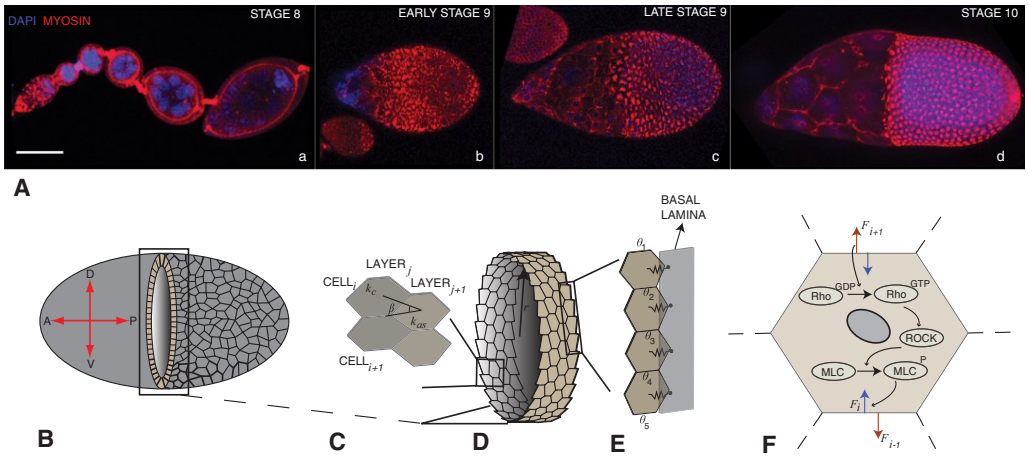


FIGURE 1: (A) (a–d) Egg chambers labeled with 4′,6-diamidino-2-phenylindole and myosin-mCherry (surface view) at stage 8 (a), early stage 9 (b), late stage 9 (c), and stage 10 (d). Maximum-intensity projection of the *z*-stacks shows the early-stage apical concentrated myosin and basal accumulation of myosin after stage 9. Scale bar, 50 μm. (B) Mechanical model. Cartoon of surface view of a *Drosophila* egg chamber showing the D-V and A-P axes. Cells are modeled as springs of stiffness $k_c$ in the D-V direction and are connected in the A-P direction through angular springs of stiffness $k_{as}$ and preferred angle β as shown in C. (D) Zoomed-in midsection of the egg chamber. (E) Connection to the basal lamina. Each cell is identified by the angular positions of its ends, $\theta$. (F) Biochemical model. Molecular pathway governing the activation of myosin contraction in response to tension. $F_i$ (blue arrow) represents contractile force from the *i*th cell, and $F_{i-1}$ and $F_{i+1}$ (red arrows) represent forces on the *i*th cell by neighboring cells.

tension and cell contractility leads to oscillations. Our model is based on the hypothesis that pressure on cells in the epithelium exerted by the growing germline cells induces the activation of the Rho-ROCK pathway (Amano *et al.*, 1997; Pellegrin and Mellor, 2007; Zhao *et al.*, 2007), which leads to negative feedback in the form of myosin contractility. We model a section of the egg chamber as circular arrays of cells connected to each other in a staggered manner (Figure 1, C–E). Cells are coupled mechanically to each other, as well as to the basal lamina, through mechanical springs in the circumferential and radial direction and angular springs in the axial direction. Forces developed by follicle cells are also under biochemical regulation. We investigate the interplay of biochemical signaling and mechanical forces during follicle cell length oscillations. The model predicts that the internal pressure of the egg chamber influences contractility of follicle cells. During egg chamber growth, increasing chamber pressure increases stress fiber formation and myosin contractility. Because cells are also mechanically coupled to each other, oscillations in any single cell are also coupled to oscillations in neighboring cells. Depending on parameters, oscillations could in principle become synchronized. However, since only asynchronous oscillations are observed experimentally, the model suggests the ranges of pressure and contractile forces that are consistent with these observations.

The model predicts that the basal lamina serves a mechanical role in egg chamber development and affects both the size of the egg chamber and the periodicity of follicle cell oscillations. Without the basal lamina, the oscillation period should become longer. We tested these predictions by removing the basal lamina using collagenase and observed an increase in the average oscillation period. We also use the model to examine mutants in which some of the follicle cells do not exert contractile force. This simulated mosaic epithelium also exhibits oscillations with properties consistent with experimental observations. Taken together, the model identifies important mechanochemical variables within the developing egg chamber and presents a quantitative understanding of active forces within the epithelial layer. The model also shows that the interplay between mechanical forces and biochemical signaling pathways is sufficient in principle to explain the spatial and temporal patterning of myosin oscillations independent of gene expression, suggesting a novel patterning mechanism during tissue morphogenesis.

## MODEL

Experiments show that basal surface area oscillations in the follicle cells during stages 9–10 of egg chamber development are mostly in the dorsal-ventral (D-V) axis direction (He, Wang, *et al.*, 2010). Based on this, a cross-section of the egg chamber with unit cell width and radius *r* is represented by a circular array of cells. A change in the basal cell surface area is modeled as a change in the cell length in the D-V direction. The length of each cell is described by angular positions of the cell edges, that is, the length of the *i*th cell is $r(\theta_{i+1} - \theta_i)$. We also assume that the passive cell behaves elastically with stiffness $k_c$. Experiments show that D-V oscillations are driven by periodic assembly and activation of myosin on actin stress fibers at the basal surface. Therefore we model this actomyosin contraction in the *i*th cell as an active force, $F_i$, contracting the cell length (Figure 1F). Interaction between two cell layers in the anterior-posterior (A-P) direction is modeled as elastic. When a cell contracts, it exerts mechanical forces on it neighbors. We model this passive mechanical interaction between cells using angular springs (Figure 1C).

In the egg chamber, follicle cells are physically adhered to the basal lamina. Therefore, when the cells contract in the D-V direction, they exert an inward radial pulling force on the membrane. We neglect the relative motion between the follicular epithelium and the basal lamina and model the deformation of the basal lamina using radial springs with stiffness *k*. Finally, it is known that the egg chamber is also under expansive internal pressure, probably from germline growth and the mechanics of nurse cells and oocyte within the epithelium. We include this pressure in the model using the parameter *P*.

Experiments show that increased contraction is correlated with increased myosin accumulation within stress fibers at the basal

surface. Therefore the biochemistry of myosin activity likely regulates active contraction of the follicle cells. In addition, the period of cell contraction is on the order of several minutes. This time scale is two orders of magnitude longer than the time scale of myosin binding and unbinding to actin, which occurs within seconds. Moreover, inhibition of Rho or ROCK prevents myosin assembly and contraction, whereas constitutive activation of Rho causes constitutive assembly and locks myosin in the fully assembled and contractile state (He, Wang, *et al.*, 2010). Therefore mechanochemical aspects of Rho-ROCK signaling are probably key to understanding D-V oscillations. It is known that when a cell is under tension (here, mostly due to mechanical tension from internal pressure), Rho becomes activated within several minutes (Zhao *et al.*, 2007). Rho activates ROCK, a protein kinase that further phosphorylates myosin light chain (MLC; Maruthamuthu *et al.*, 2011; Bhadriraju *et al.*, 2007), leading to myosin contraction. We assume that the contractile force is directly proportional to the fraction of activated myosin. The modeled signaling pathway is shown in Figure 1F.

### Mechanical model

For a cross-section of unit cell width as in Figure 1E, motions of the cell ends in the $r$ and $\theta$ directions can be obtained from a mechanical energy formulation of the cell layer. This energy is a sum of the elastic energies—from follicle cells, as well as the connectors to the basal lamina—the work done by the actomyosin contractile force, and the work done by pressure $P$ inside the egg chamber. The mechanical energy per length is then

$$E = \underbrace{\sum_{i=1}^{N} \frac{1}{2} k_c (r(\theta_{i+1} - \theta_i) - l_o)^2}_{\text{Cell length}} + \underbrace{\frac{1}{2} Nk (r - r_o)^2}_{\text{Basal lamina}}$$

$$- \underbrace{\sum_{i=1}^{N} F_i r(\theta_{i+1} - \theta_i)}_{\text{Contractile force}} - \underbrace{P\pi r^2}_{\text{Pressure-volume}} \qquad (1)$$

where $r$ is the radius of the circular cell array and is assumed to be the same for all the cells, $l_o$ is the rest length of the cell, $N$ is the number of cells in a cross-section, $Nk$ is the effective stiffness of the basal lamina, and $r_o$ is the preferred basal lamina radius.

At the scale of the egg chamber, inertia is unimportant, and forces are balanced by friction. Equations of motion for $r$ and $\theta_i$ can be obtained from the mechanical energy by differentiating with respect to these variables and equating them to friction. The details are given in Eqs. 2 and 3 in the Supplemental Material. Thus we propose that in the absence of cellular contractile forces, follicles cells are stretched by internal pressure, $P$. We propose that the cells generate contractile force that opposes the egg chamber pressure, and it is the biochemical control of the contractile stress that generates oscillations.

### Biochemical model

Models of Rho-ROCK signaling pathway have been studied before (Civelekoglu-Scholey *et al.*, 2005; Jilkine *et al.*, 2007). Here we propose a model in which the activation of Rho and myosin is related to mechanical tension in the cell. Increased activation of Rho, ROCK, and MLC in tissue cells in response to external tension has been observed (Zhao *et al.*, 2007). We propose that this also occurs in follicle cells. The kinetics of Rho, ROCK, and MLC activation in the $i$th cell are modeled as

$$\frac{d\rho_i}{dt} = f_\rho(s_i)(1 - \rho_i) - D_\rho \rho_i \qquad (2)$$

$$\frac{dR_i}{dt} = f_R(\rho_i)(1 - R_i) - D_R R_i \qquad (3)$$

$$\frac{dm_i}{dt} = f_m(R_i)(1 - m_i) - D_m m_i \qquad (4)$$

where $\rho_i$, $R_i$, and $m_i$ represent the fraction of activated Rho, ROCK, and MLC respectively, and $s_i$ is the change in length of the $i$th cell, $r(\theta_{i+1} - \theta_i) - l_o$; the mechanical tension is then $k_c s_i$. Every rate equation has an activation and a deactivation part. The deactivation part is linear, which can represent any number of biochemical mechanisms, such as hydrolysis of $Rho^{GTP}$ to $Rho^{GDP}$ or constitutive phosphatase activity that inactivates ROCK. In the activation part, $f_\rho(s)$ represents the effect of the mechanical tension on the activation of Rho. Similarly $f_R(\rho)$ and $f_m(R)$ represent the effect of Rho on ROCK and the effect of ROCK on MLC, respectively. Mathematically, nonlinearity in the system is one way to obtain sustained oscillations (Ferrel *et al.*, 2011). We incorporate nonlinearity in the form of a Hill function for the effect of tension on the activation of Rho, representing possible cooperativity in Rho activation:

$$f_\rho(s) = A_\rho h(s) \frac{s^n}{K_s + s^n} (1 - \rho) \qquad (5)$$

$$f_R(\rho) = A_R \rho \qquad (6)$$

$$f_m(R) = A_m R \qquad (7)$$

$h$ is a Heaviside step function, which is 0 when $s$ is negative and 1 when $s$ is positive. This ensures that Rho is activated upon cell stretching under tension. $A_\rho$, $A_R$, and $A_m$ are the rates of activation, and $D_\rho$, $D_R$, and $D_m$ are the rates of deactivation. $K_s$ is the half-maximal response constant, and $n$ is the Hill coefficient for cooperativity.

Because the contractile force $F$ originates from the activation of MLC, we can assume that the force is linearly proportional to the fraction of activated MLC. The proportionality constant, $F_{max}$, represents the contractile force of a cell when the activated myosin fraction is 1, that is, the maximum contractile force:

$$F_i(t) = -F_{max} m_i(t) \qquad (8)$$

$F_{max}$ is related to the total amount of contractile myosin available for the basal stress fibers, whereas $F_i$ is related to the amount of activated myosin generating contractile force within the stress fibers. Note that the proposed mechanical signaling model explains why stress fibers and contractile force are in the D-V direction in follicle cells. For an approximately cylindrical egg chamber, the mechanical tension from the internal pressure $P$ is $Pr$ in the D-V direction and $Pr/2$ in the A-P direction. Therefore, for the same internal pressure, Rho activation and stress-fiber formation would occur in the D-V direction first. The internal pressure and the shape of the egg chamber determine the direction of oscillation.

In the biochemical model (Eq. 5), the form of tension-activated kinetics is not essential. In the Supplemental Material, we examine a simpler model in which $f_\rho(s) = A_\rho h(s) s$. This linear function can still produce similar oscillatory dynamics. In general, oscillations can occur when there is a time delay in the coupled dynamics in the system. Here the mechanical time scale, $\gamma/k_c$, is similar to the time scale of biochemical kinetics. This provides the necessary time delay to generate oscillations in contraction.

### Two-dimensional epithelial layer

In the egg chamber, follicle cells form the epithelial sheet; therefore cells are coupled in the D-V circumferential direction as well as in

the A-P direction (Figure 1D). We model A-P mechanical coupling using angular springs. Therefore the total energy of the epithelial sheet is

$$E = \sum_{j=1}^{n}\sum_{i=1}^{N_j}\frac{1}{2}k_c(r(\theta_{j,i+1}-\theta_{j,i})-l_o)^2 - F_{j,i}r(\theta_{j,i+1}-\theta_{j,i}) + E_{\text{bl}} + E_{\text{as}} - ndP\pi r^2 \quad (9)$$

$$E_{\text{bl}} = \sum_{j=1}^{n}\frac{1}{2}N_j k(r-r_o)^2 \quad (10)$$

$$E_{\text{as}} = \sum_{j=1}^{n}\sum_{i=1}^{N_j}\frac{1}{2}k_{\text{as}}(\beta_{j,i}-\beta_o)^2 \quad (11)$$

$$\beta_{j,i} = \arctan\left[\frac{r((\theta_{j+1,i+1}-\theta_{j+1,i})-(\theta_{j,i+1}-\theta_{j,i}))}{d}\right] \quad (12)$$

where $j$ labels the row in the A-P direction and $i$ labels the cell in the same row in the D-V direction; $E_{\text{bl}}$ is the energy of the mechanical springs connecting cells to the basal lamina, and $n$ is the number of cell rows. $E_{\text{as}}$ is the energy corresponding to the angular springs (of stiffness $k_{\text{as}}$) connecting different layers, $N_j$ is the number of cells in the $j$th row, β is the angle made by angular springs with the horizontal, and $d$ is the distance between rows, which would correspond to typical cell width (Figure 1). $\beta_o$ is the preferred angle between cells in adjacent rows.

In this model, we assume that the cell–cell connections between rows are fixed, that is, the interactions are not dynamic. In reality, the connections are made through cadherin bonds, and there is an adhesion component as well as a shear/friction component. We neglected the shear component because the differences in angular velocities between rows are small. Therefore relative sliding of cells in adjacent rows is negligible.

## RESULTS

### Single cell oscillates under mechanical stretch

The simplest case is when a single follicle cell is under tension. This case is not possible to examine in experiments, but it is possible to explore using our model. Figure 2 shows an example in which an externally applied force stretches a single cell and the force gradually increases with time (Figure 2A). Our model predicts that the cell length will increase with increasing applied force (Figure 2B); however, activated Rho will also increase with increasing applied force (Figure 2C). The activated Rho catalyzes activation of myosin in the stress fibers, and the cellular contractile force increases to oppose the applied force. Within a range of applied force, the Rho-ROCK signaling network exhibits oscillations. This oscillation is a limit cycle (Figure 2E). The period of oscillation depends on the rate of Rho and ROCK activation. An analytical estimate of the oscillation period is given in the Supplemental Material (Supplemental Figures S4 and S5).

### Asynchronous oscillations in cell D-V length and myosin content and factors influencing frequency in the multicell model

When multiple follicle cells are mechanically connected in the epithelium, our model simulations show that the cells will oscillate along the D-V axis with an average period of ~5–7 min (He, Wang, *et al.*, 2010). The oscillation amplitude ranges from 0.5 to 2 μm, which also is what experiments observe (He, Wang, *et al.*, 2010). Experiments show that oscillations in myosin intensity are correlated with and precede oscillations in basal cell area in follicle cells (He, Wang, *et al.*, 2010). In our model, normalized activated myosin also

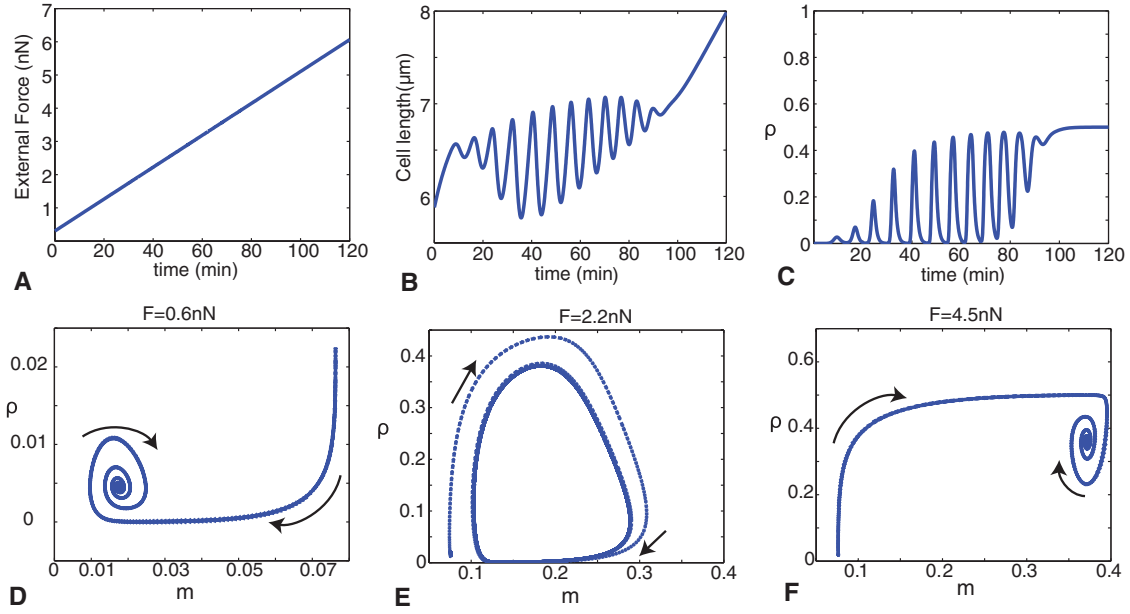


FIGURE 2: Behavior of single follicle cells. (A) As we apply an increasing external stretching force to a single follicle cell, we see that (B) the follicle cell length increases with increasing force. However, as the force reaches a threshold, the cell starts to oscillate. At large forces the oscillations disappear and the cell continues to stretch. (C) The amount of activated Rho increases with increasing force, and there is an oscillation in the amount activated Rho. Rho reaches a maximum value at large force. (D–F) When the external force is held constant, three behaviors are seen. At low forces (D), the system settles to a steady level of activated Rho and MLC. At intermediate forces (E), the system exhibits an oscillatory limit cycle. At high forces (F), a steady state is again reached. Therefore our model predicts a Hopf bifurcation with increasing external force.

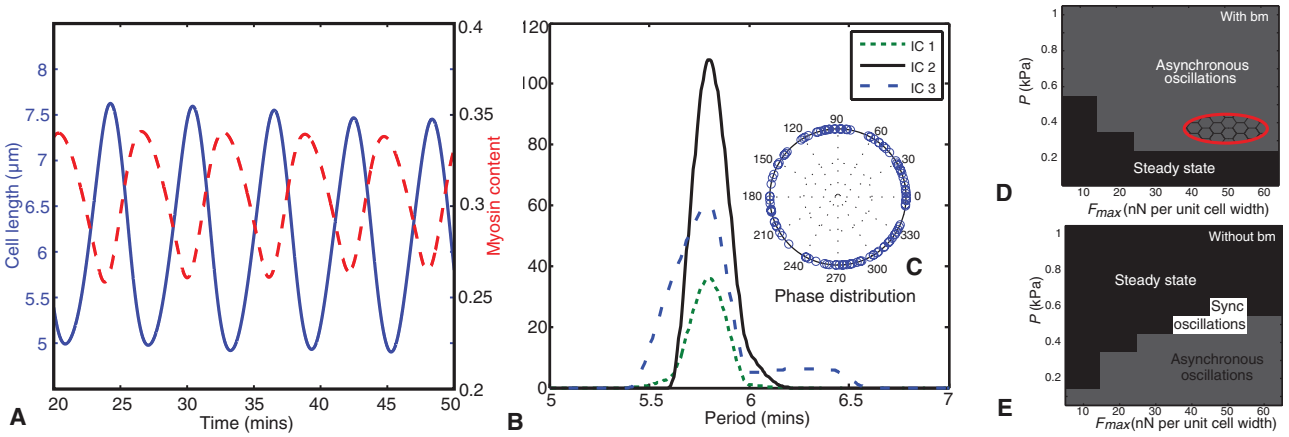


FIGURE 3: Follicle cell length and myosin oscillations. (A) Plot showing oscillations in cell length (blue) and myosin content (red). Increase in myosin content corresponds to decrease in cell length. (B) Oscillation period distribution for different initial conditions (ICs), showing that the range is between 5 and 7 min and is independent of ICs. (C) Phase distribution of oscillations in 120 cells, showing that the oscillations are asynchronous. The phases are uniformly distributed around $2\pi$. (D, E) Phase diagrams of oscillatory behavior with and without basal lamina. The system generally exhibits asynchronous oscillations or steady nonoscillatory behavior. There is a small synchronous oscillation regime without basal lamina (white), although this would require a high internal pressure. The red circle indicates, in our model, the region close to the physiological situation.

shows oscillations with periods similar to those of oscillations in cell length. Figure 3A shows myosin and cell length oscillations on the same plot. Myosin activation precedes reduction in cell length as observed in vivo. We fit a cosine function to the computed oscillations and obtain the phase of oscillation for each cell. We find that this system at long times shows a uniform distribution of oscillatory phase (Figure 3C). This suggests that the oscillations are asynchronous. If oscillations are synchronous, all cells would have a similar phase, and the phase distribution would be more concentrated. We do find a synchronous phase in other parameter regimes (Figure 3, D and E). The observed oscillations are also independent of initial starting configurations of the model (Figure 3B).

$F_{max}$ and $P$ are the important physical variables in this system. $F_{max}$ is the maximum possible myosin contractile force, representing maximum activation of myosin. $P$ is the internal egg chamber pressure. The pressure generates a tension of $T = Pr$ in the D-V direction of the epithelial layer. In response to this tension, cells activate myosin contraction to balance this tension. Note that there is also a tension in the A-P direction, but it is half of the tension in the D-V direction. Because increasing tension increases myosin activation, our model also predicts that the radius of the egg chamber will influence the observed myosin intensity (Supplemental Figure S2). Indeed, we see that the combination of egg chamber pressure, geometry, and epithelial tension is another mechanism of spatial pattern formation. Myosin activation responds nonlinearly to tension, and larger egg chamber radius will lead to a stronger activation. In an egg chamber with spatially varying radius but uniform pressure, myosin will become activated first in regions of larger radius.

Computations show that frequency and amplitude of cell oscillations, as well as the egg chamber radius and mean myosin intensity, all depend on $F_{max}$ and $P$ (Supplemental Figures S6 and S7). In particular, the egg chamber radius decreases with increase in the maximum contractile force $F_{max}$ and increases with increase in internal egg chamber pressure $P$ (Figure 4). Oscillation period follows a decreasing trend with increase in $F_{max}$. For some parameter regimes, synchronized oscillations are also seen. We estimate that physiologically relevant parameters are close to $F_{max} = 50$ nN and $P = 0.3$ kPa.

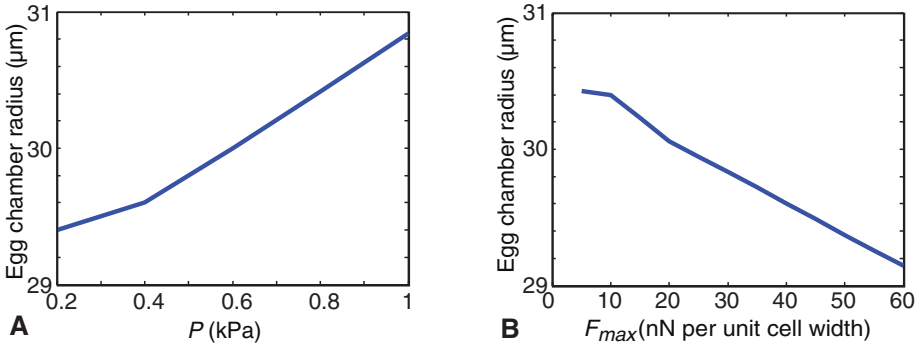


FIGURE 4: Internal egg chamber pressure and maximum contractile force have opposing effects on egg chamber radius. (A) Plot showing change in egg chamber radius as a function of internal pressure ($P$). Increase in pressure increases the egg chamber radius (here $F_{max} = 40$nN per unit-cell width). (B) Plot showing change in egg chamber radius as a function of maximum contractile force $F_{max}$. Increase in $F_{max}$ decreases the egg chamber radius (here $P = 0.4$ kPa).

We further investigated the effect of ROCK activation and the radius of the egg chamber on the oscillation period. In experiments, it is possible to interfere with the activity of ROCK using Y-27632, a ROCK inhibitor. It was found that at inhibitor doses at which oscillations persisted, the period largely remained unchanged. We model this experiment by varying ROCK activation rate, $A_R$, in Eq. 6, and observe a similar behavior. We still see oscillations, and the oscillatory period depends nonmonotonically on $A_R$ (Supplemental Figure S3). The egg chamber radius does affect oscillation period. For smaller radii, higher contractile force is required to cause oscillations, whereas at larger radii, higher pressures induce oscillations (Supplemental Figure S6D).

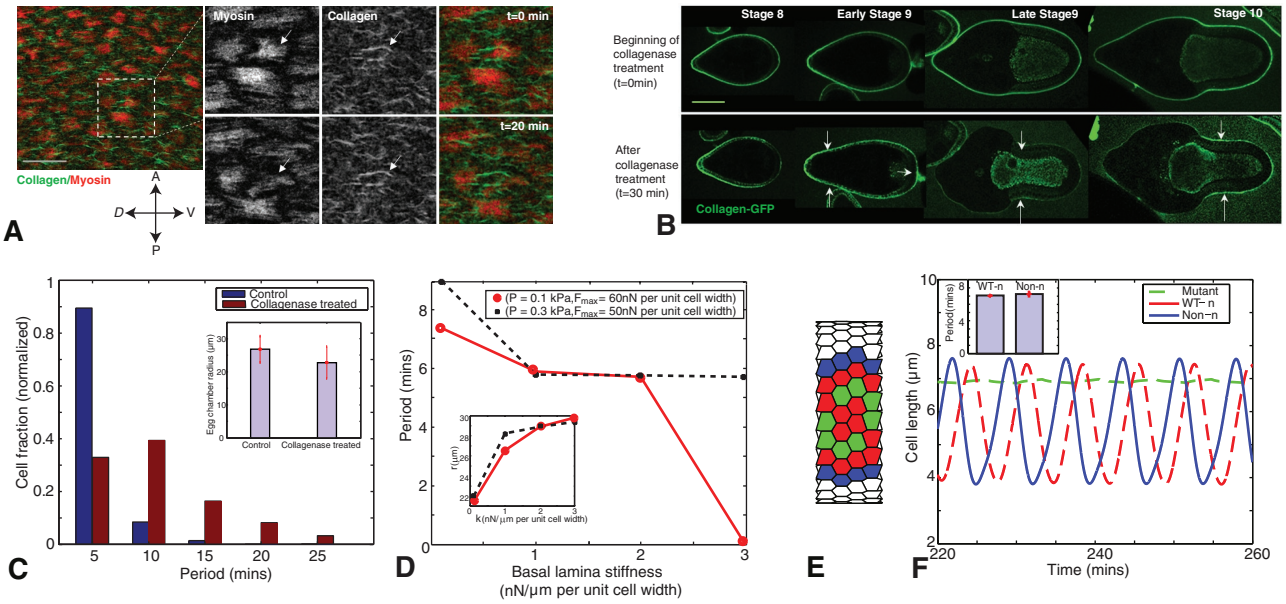


FIGURE 5: Effects of the basal lamina and mosaic analysis. (A) Images of basal lamina (labeled with collagen–green fluorescent protein [GFP]) and myosin (myosin-mCherry) in control conditions. The relative positions of collagen and myosin fibers remains unchanged, suggesting that basal lamina could be mechanically coupled to basal myosin. Scale bar, 20 μm. (B) Egg chambers stained with collagen-GFP from stage 8 to stage 10 in control conditions, at the beginning of collagenase treatment ($t = 0$ min), and after collagenase treatment ($t = 30$ min). (C) Experimental measurements on follicle oscillations upon disruption of basal lamina. The distribution of oscillation periods became longer. The average egg chamber width became smaller (inset). (D) Modeling predictions of oscillation period as a function of stiffness of the basal lamina. Collagenase treatment reduces basal lamina stiffness and increases oscillation period for several values of $P$ and $F_{max}$. The predicted egg chamber radius also becomes smaller as basal lamina stiffness is reduced, in agreement with experiments. (E) It is possible to abolish myosin contraction in some follicle cells using constitutively relaxing cells (ROCK RNAi–expressing cells); these cells (green) do not oscillate. It is then possible to examine the interaction between the wild-type cells (blue and red) and mutant cells (green). (F) Experiments and modeling show that there are no changes to oscillatory period in neighboring wild-type cells (blue) or wild-type cells directly neighboring mutant cells (green). Mutant cells, however, cease to oscillate. The oscillatory period is unchanged in neighboring versus nonneighboring wild-type cells (inset).

## The basal lamina plays a role in determining periodicity of follicle cell oscillations

In the egg chamber, the basal lamina is a highly cross-linked and complex structure, with collagens comprising ~50% of the protein (Kalluri, 2003). Follicle cells adhere to the basal lamina via integrin-mediated adhesions that contain focal adhesion proteins such as talin and paxillin (Figure 5A and Supplemental Figure S8). We examined the effect of the basal lamina on follicle cell oscillations by treating wild-type cells with collagenase to partially remove the basal lamina surrounding the egg chamber (Figure 5B). Figure 5C shows the distribution of oscillation periods for control and collagenase-treated samples. On collagenase treatment, some cells no longer exhibit oscillations. Other cells show an increased oscillation period. The mean period in the control condition is 5.6 min, which increases to 10.6 min. In addition, the egg chamber radius decreases by ~20% upon collagenase treatment (Figure 5C, inset).

In our model, we can examine the effects of the basal lamina by varying the stiffness of the mechanical spring connecting the epithelial layer to the basal lamina ($k$). We decreased $k$ from 3 to 0.1 nN/μm per unit-cell width in the simulations. In Figure 5D, oscillation period is shown as a function of $k$. The general trend in the $P$–$F_{max}$ space is an increase in oscillation period as the stiffness decreases. In one of the cases, $P = 0.1$ kPa, $F_{max} = 60$ nN per unit-cell width (red), the system starts from a steady state and goes to an oscillatory phase with increasing period as stiffness decreases. In the other case shown (black), at $P = 0.3$ kPa, $F_{max} = 50$ nN per unit-cell width, the system shows a gradual increase in oscillation period as stiffness decreases.

## Autonomy of cell oscillations

Experimentally, wild-type cells surrounded by either constitutively relaxing cells (ROCK RNA interference–expressing cells) or with constitutively contracting cells (Rho V14–expressing cells) still oscillate with normal amplitude and period, indicating that these oscillations are cell autonomous (He, Wang, *et al.*, 2010). We checked this in our simulations by surrounding wild-type cells with those having no active Rho and ROCK (Figure 5, E and F). There seems to be no difference in period in neighboring and nonneighboring wild-type cells, as seen in experiments (He, Wang, *et al.*, 2010).

## Other model predictions

If all cells exert the same contractile force and contractions are synchronized, then the forces exactly balance and there is no net torque on the egg chamber. However, because the oscillations are not synchronized, the net torque in the system is not exactly zero. Our simulations predict that if we incorporate shear motion between the basal lamina and the epithelial layer, the net torque will cause an overall rotation in the egg chamber against the basal lamina. This overall egg chamber rotation has been observed (Haigo and Bilder, 2011). In addition, buildup of stress fibers and oscillations of follicle

cells start from the middle of the egg chamber, where the radius is largest. As the chamber grows larger, the oscillatory region grows to encompass the whole epithelial layer. This is consistent with our tension-activated model because mechanical tension is directly proportional to chamber radius. For the same internal pressure, larger radius will activate Rho and myosin contraction first.

## DISCUSSION

We introduced a mechanochemical model of follicle cell oscillation in the developing *Drosophila* egg chamber. The model describes the response of follicle cells to external forces and how egg chamber mechanics can potentially influence biochemical signaling and contractile force generation. In particular, we suggest that the egg chamber is under internal pressure, and follicle cells, together with the basal lamina, exert forces to balance the expansionary pressure. During egg chamber growth, the pressure gradually increases, leading to an increasing follicle cell contractile force. Eventually, the system undergoes a Hopf bifurcation with the egg chamber pressure as the critical parameter, and oscillations in contraction appear. We showed that the observed oscillations are not synchronized and mechanical properties of the basal lamina can influence the frequency of oscillations.

In this article we focused on biochemical regulation of contraction by the Rho signaling pathway. This is because the time scale of oscillation is on the order of minutes, much longer than the time scale of myosin interacting with actin (seconds). Estimates of Rho activation rates are consistent with the oscillation period (Zhang and Zheng, 1998). However, the time scale of stress fiber formation in actin networks under force is also on the order of minutes (Walcott and Sun, 2010). Experiments have shown that Rho is necessary for the observed autonomous contraction, and therefore we focused on this pathway. Mathematical modeling of stress-fiber formation based on adhesion formation and Rho-ROCK signaling also suggests a similar time scale (Civelekoglu-Scholey *et al.*, 2005). Here we focus on the process of Rho activation arising from cell tension. We also used a simplified two-dimensional description of follicle cells mechanics. Three-dimensional (3D) mechanical models of epithelial cell morphology have been proposed (Hannezo *et al.*, 2014). Our model can be extended to the 3D regime by incorporating 3D cell shapes.

The proposed biochemical signaling model controlling cell contractility may have implications in other tissue cells. The model suggests that as external forces stretch the cell, the tension in the cell cortex or membrane increases. This triggers a cooperative activation of Rho GTPase and ROCK, leading to a cascade of phosphorylation events that eventually activates myosin light chain, stress-fiber formation, and contractile force generation. This type of tension-activated contractile force generation has been observed in fibroblasts (Zhao *et al.*, 2007). Therefore the basic framework of the model will likely apply to other cells and tissues.

The prevailing view of tissue development is that morphogens pattern cell fates and gene expression, which in turn determine patterns of differential mechanical properties that drive major morphogenetic events such as invagination during gastrulation or convergence and extension movements (Zallen and Wieschaus, 2004; Lecuit and Lenne, 2007; Martin *et al.*, 2009). Patterns of active contractile forces are clearly an important element throughout morphogenesis (Jacinto *et al.*, 2002; Berg, 2008; Martin *et al.*, 2010). Here we show that patterns of actomyosin contractility can in principle emerge from mechanochemical interactions alone, without an initiating event based on a pattern of gene expression or a morphogen signal. These active tissue contractions help to maintain mechanical tension in the epithelia and pressure within the egg chamber and also the geometry of the egg chamber. It will be interesting to determine whether this is a widespread mechanism that shapes organs and tissues.

## MATERIALS AND METHODS

### Mathematical model

Our model has four cross-sections (circular arrays of cells) stitched together into a cylindrical sheet; each cross-section has 30 cells, for a total of 120 cells in the system. Each cell has four equations corresponding to four variables: angular position and activated Rho, ROCK, and MLC fractions. In addition, there is one equation for the radius of the egg chamber. We solve this set of 481 differential equations simultaneously using MATLAB's (MathWorks, Natick, MA) ode45 for a time period of ~5 h. Periodic boundary conditions are used. The initial conditions are generated randomly with the following constraints. The Rho, ROCK, and MLC fractions are <1, and the angular positions of cells (begin and end positions) are chosen such the sum of all the angular cell lengths equals $2\pi$. Additional model details and parameters used in the computation are given in the Supplemental Material (Tables S1 and S2).

### Data analysis from experiments

***Fly stocks***. The following fly stocks were used in this work: UAS-GFP-Paxillin, Ubi::DE-Cadherin-GFP, sqh::sqh-mcherry (from Eric F. Wieschaus, Department of Molecular Biology, Princeton University, Princeton, NJ), Talin-EGFP (MiMiC fly from Hugo Bellen, Baylor College of Medicine, Duncan Neurological Research Institute, Houston, TX), and Viking-GFP (from David Bilder, Department of Molecular and Cell Biology, University of California, Berkeley, Berkeley, CA). All stocks and crosses were maintained at room temperature. Female flies, 3–7 d posteclosion, were used for the experiment.

***Live imaging and chemical treatment***. Live imaging of the *Drosophila* egg chamber was done as previously described (Prasad *et al.*, 2007). Time-lapse imaging was carried out on either a Zeiss (Oberkochen, Germany) 710 NLO confocal microscope using a 40×/numerical aperture (NA) 1.1 water immersion lens or an Olympus (Shinjuku, Tokyo, Japan) FV1200 confocal microscope with 40×/NA 1.25 oil immersion lens. *Z*-stacks with two or three slices (3 µm in thickness) were taken to capture the entire basal myosin. The maximum-intensity projected images were used for analysis. In chemical treatment experiment, egg chambers were first dissected in live imaging medium. Then the dissection medium was removed and replaced by medium containing collagenase (1 mg/ml; Sigma-Aldrich, St. Louis, MO), latrunculin A (100 µM; Sigma-Aldrich), or ionomycin (2.5 µM; Invitrogen Life technologies, Carlsbad, CA). Then egg chambers were either mounted immediately for live imaging or incubated in the medium for 1 h before quantification. We used 4% formaldehyde for fixative and Alexa 569–conjugated phalloidin (1:300, Invitrogen) for F-actin staining.

***Image analysis of fly movies***. Live *Drosophila* egg chamber movies, imaged at 60-s intervals for 1 h during stage 10A, were analyzed to calculate oscillation period. Myosin intensity was calculated as follows. The myosin-labeled images were first filtered using a Gaussian blur filter with a radius of 25 pixels in ImageJ. These images were then subtracted from the originals as background. After enhancing contrast, the images were segmented using a software ilastik (Sommer *et al.*, 2011). Segmented images were manually checked for errors using Photoshop and analyzed using MATLAB for

myosin intensity and cell area measurements. The myosin intensity was normalized with respect to maximum value for each of the frames and plotted as a function of time in Supplemental Figure S1. Myosin intensity measurements were used to calculate oscillation period using autocorrelation, as they were less noisy than the surface area data. Distances between peaks in the autocorrelation plot of myosin intensity give the period distribution. A total of 87 cells in the control condition and 91 cells in the collagenase-treated condition were analyzed to calculate the period in each case.

## ACKNOWLEDGMENTS

This work was supported by National Institutes of Health Grants 1U54CA143868-01, R01GM73164, and 1R01GM075305 and National Science Foundation Grant PHY-1205795.

## REFERENCES

Boldface names denote co–first authors.

Amano M, Chihara K, Kimura K, Fukata Y, Nakamura N, Matsuura Y, Kaibuchi K (1997). Formation of actin stress fibers and focal adhesions enhanced by Rho-kinase. Science 275, 1308–1311.

Berg CA (2008). Tube formation in *Drosophila* egg chambers. Tissue Eng Part A 14, 1479–1488.

Bhadriraju K, Yang M, Alom Ruiz S, Pirone D, Tan J, Chen CS (2007). Activation of ROCK by RhoA is regulated by cell adhesion, shape, and cytoskeletal tension. Exp Cell Res 313, 3616–3623.

Civelekoglu-Scholey G, Orr AW, Novak I, Meister JJ, Schwartz MA, Mogilner A (2005). Model of coupled transient changes of Rac, Rho, adhesions and stress fibers alignment in endothelial cells responding to shear stress. J Theor Biol 232, 569–585.

Ferrell JE Jr, Tsai TY, Yang Q (2011). Modeling the cell cycle: why do certain circuits oscillate? Cell 144, 874–885.

Goldbeter A (1996). Biochemical Oscillations and Cellular Rhythms: The Molecular Bases of Periodic and Chaotic Behaviour, Cambridge, UK: Cambridge University Press.

Haigo SL, Bilder D (2011). Global tissue revolutions in a morphogenetic movement controlling elongation. Science 331, 1071–1074.

Hannezo E, Jacques P, Joanny J-F (2014). Theory of epithelial sheet morphology in three dimensions. Proc Natl Acad Sci USA 111, 27–32.

**He L**, **Wang X**, Tang HL, Montell DJ (2010). Tissue elongation requires oscillating contractions of a basal actomyosin network. Nat Cell Biol 12, 1133–1142.

Jacinto A, Woolner S, Martin P (2002). Dynamic analysis of dorsal closure in *Drosophila*. Dev Cell 3, 9–19.

Jilkine A, Maree AF, Edelstein-Keshet L (2007). Mathematical model for spatial segregation of the Rho-family GTPases based on inhibitory crosstalk. Bull Math Biol 69, 1943–1978.

Kalluri R (2003). Basement membranes: structure, assembly and role in tumour angiogenesis. Nat Rev Cancer 3, 422–433.

Lecuit T, Lenne PF (2007). Cell surface mechanics and the control of cell shape, tissue patterns and morphogenesis. Nat Rev Mol Cell Biol 8, 633–644.

Martin AC, Gelbart M, Fernandez-Gonzalez R, Kaschube M, Wieschaus EF (2010). Integration of contractile forces during tissue invagination. J Cell Biol 188, 735–749.

Martin AC, Kaschube M, Wieschaus EF (2009). Pulsed contractions of an actin-myosin network drive apical constriction. Nature 457, 495–499.

Maruthamuthu V, Sabass B, Schwarz US, Gardel ML (2011). Cell-ECM traction force modulates endogenous tension at cell-cell contacts. Proc Natl Acad Sci USA 108, 4708–4713.

Prasad M, Jang AC, Starz-Gaiano M, Melani M, Montell DJ (2007). A protocol for culturing Drosophila melanogaster stage 9 egg chambers for live imaging. Nat Protoc 2, 2467–2473.

Pellegrin S, Mellor H (2007). Actin stress fibres. J Cell Sci 120, 3491–3499.

Sommer C, Straehle C, Kothe U, Hamprecht FA (2011). ilastik: Interactive Learning and Segmentation Toolkit. In: Eighth IEEE International Symposium on Biomedical Imaging (ISBI). Proceedings, New York: IEEE, 230–233.

Walcott S, Sun SX (2010). A mechanical model of actin stress fiber formation and substrate elasticity sensing in adherent cells. Proc Natl Acad Sci USA 107, 7757–7762.

Winfree AT (1980). The Geometry of Biological Time, Heidelberg, Germany: Springer.

Zallen JA, Wieschaus EF (2004). Patterned gene expression directs bipolar planar polarity in *Drosophila*. Dev Cell 6, 343–355.

Zhang B, Zheng Y (1998). Regulation of RhoA GTP hydrolysis by the GTPase-activating proteins p190, p50RhoGAP, Bcr, and 3BP-1. Biochemistry 37, 5249–5257.

Zhao XH, Laschinger C, Arora P, Szaszi K, Kapus A, McCulloch CA (2007). Force activates smooth muscle α-actin promoter activity through the Rho signaling pathway. J Cell Sci 120, 1801–1809.